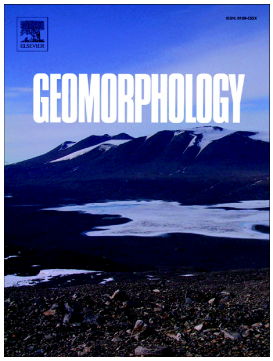

On the applicability of empirical formulas for natural salients to Sardinia (Italy) beaches

A. Sulis, A. Balzano, C. Cabras, A. Atzeni

PII: S0169-555X(16)30358-0
DOI: doi: 10.1016/j.geomorph.2017.02.025
Reference: GEOMOR 5943

To appear in: *Geomorphology*

Received date: 24 May 2016
Revised date: 27 February 2017
Accepted date: 28 February 2017

Please cite this article as: A. Sulis, A. Balzano, C. Cabras, A. Atzeni , On the applicability of empirical formulas for natural salients to Sardinia (Italy) beaches. The address for the corresponding author was captured as affiliation for all authors. Please check if appropriate. Geomor(2017), doi: 10.1016/j.geomorph.2017.02.025

On the applicability of empirical formulas for natural salients to Sardinia (Italy) beaches

Sulis, A.[1,*], Balzano, A.[2] Cabras, C.[3] and Atzeni, A.[4]

[1]Senior Consultant, University of Cagliari, Center of Environmental Sciences (CINSA)
Via S.Giorgio, 12
09123 Cagliari (CA), Italy

[2]Associate Professor, University of Cagliari, Department of Civil and Environmental Engineering and Architecture (DICAAR), Hydraulic Sector
Via Marengo, 2
09124 Cagliari (CA), Italy

[3]Graduate Student, University of Cagliari, Department of Civil and Environmental Engineering and Architecture (DICAAR), Hydraulic Sector
Via Marengo, 2
09124 Cagliari (CA), Italy

[4]Full Professor, University of Cagliari, Department of Civil and Environmental Engineering and Architecture (DICAAR), Hydraulic Sector
Via Marengo, 2
09124 Cagliari (CA), Italy

[*] Corresponding Author: asulis@unica.it

Abstract:

The paper presents an empirical analysis of the shoreline response to natural obstacles, either submerged reefs and islands, distributed along the Sardinian (Italy) coastlines exposed to different wave and wind climates. The study focuses on salient morphological features whose geometrical properties have been acquired through an extensive field and image-derived survey. The current analysis has been used to propose geometric predictive formulas for stable salients that overcome some limitations affecting previous works. A semi-probabilistic method based on well-known rate-of-change statistics is also presented to verify the equilibrium condition of

salients. Analysisresults suggest that site-specific wave transmission in the lee of submerged reefs requires a range of salient limiting B/S ratio values broader than those presented in the literature, B being the length of the obstacle and S the distance between undisturbed beach and obstacle. The B/S ratio has been proved to be the main dimensionless variable for predicting salient amplitude and basal width. In particular, the proposed predictive equation suggests an erosion condition for some combinations of B/Sand the "8 times rule" appears not to be applicable to natural salients.

Keywords*: salient, natural offshore obstacle, long-term equilibrium condition, empirical predictive formulae, Sardinia.*

INTRODUCTION

Shore-parallel structures in the form of rubble-mound emergent breakwaters located within the surf zone are the most common protective structures for limiting shoreline erosion or for promoting beach widening. In contrast, fully submerged (Ranasinghe and Turner, 2006) and low-crested (Lamberti and Zanuttigh, 2009) structures have only rarely been adopted for beach protection. A critical aspect in the design of these breakwaters is the prediction of the effects of the structures on the shoreline. Often, incorrectly dimensioned breakwaters can result in the formation of an unwanted tombolo and/or an eroding downdrift beach. Engineers and scientists have predicted long-term shoreline evolution in the lee of an offshore obstacle primarily using a) physical models, b) models based on the conservation of

sand volume equation (one-line models), c) coastal morphodynamics models, and d) empirical models. Physical models (see e.g. Mory and Hamm, 1997) are well-suited to local analysis but are cost prohibitive to use for very large scales and their applicability is constrained by scaling problems for the sediment. The conservation-of-sand-volume approach, also known as the "one-line approach", has become the preferred modeling approach for evaluating shoreline change that could result from anthropogenic or natural changes in the beach and seaward salients system present in a coastal area. All one-line models assume the beach profile shape remains constant, the shoreward and seaward vertical limits of the profile are constant, the sand is transported alongshore by the action of breaking waves and longshore currents, the detailed structure of the nearshore circulation is ignored, and there is a long-term trend in shoreline evolution due to an infinite supply of sand. Examples of one-line models are GENESIS (Hanson and Kraus, 2011) or LITPACK by DHI. Numerical models of the equations of shoreline and beach motions are implemented in models of coastal morphodynamics in simple or more complete form, but these require large computational resources and are not well-suited to the large spatial and temporal scales over which beaches and nearshore salients evolve. These coastal morphodynamic models are further subdivided into two-dimensional horizontal models (e.g. Ranasinghe et al., 2006), which use depth-averaged equations, and three-dimensional models (e.g. Lesser et al., 2004), which resolve the vertical variations in flow and transport. Large differences exist in the type of wave, flow and sediment transport models applied, the frequency of updating, numerical bed updating schemes and

morphological acceleration techniques. Roelvink and Reniers (2012) provide a review of different numerical schemes implemented in these models, with an in-depth discussion of strong points and hindrances of the each model for simulating different coastal processes. Empirical models are formulated as simple relations between the obstacle geometry and the resulting shoreline evolution. To define empirical predictive formulas, models use wave diffraction theoryto predict an equilibrium shoreline (Hsu et al., 2003), and are based on analysis of field data (Hsu and Silvester, 1990) or results from numerical models (Hakeem et al., 2010). Empirical predictive formulas are reasonably in agreement with numerical model results (Kristensen et al., 2013)and can provide a complementary tool with morphodynamic models that uses implified input data to obtain reliable results, as demonstrated by Sulis and Annis (2014) in the application of the uncoupled morphological model of the package MIKE 21 FM (DHI, 2008) to theshoreline stability of a salient in the lee of an emergent natural reef at Sa Mesa Longa (Sardinia).The ability of empirical predictive formulas to predict the characteristics of shoreline salients has a clear engineering relevance. Practicing engineers often have to provide solutions to beach protection and these empirical formulas can provide a conservative approach to the preliminary characterization of the shoreline evolution behind the designed structure. Therefore, the empirical approach is not intended to support further engineering design in more advanced levels as, at that step, detailed field survey data are available to feed accurate morphodynamic models. The practical utility of these predictive equations is in assisting coastal engineers to roughly estimate the geometric values of

the main governing parameters at a preliminary design level (Hsu and Evans, 1989).

Shoreline salients are often observed in the lee of natural reefs located in the nearshore region. To date, no systematic studies on the effects of natural obstacles, either submerged reefs or islands, have been undertaken along the Mediterranean coasts to provide empirical predictive formulas. Particularly, reasonable quantitative relationships for determining the geometrical properties of shoreline adjustment to natural obstacles are lacking. Black and Andrews (2001) defined criteria for salient formation and empirical relationships to describe the morphology of salients and their geometries by visually inspecting aerial photographs of the coastlines of southeastern Australia and New Zealand. However, some of the conclusions from this study are counter-intuitive, and Ranasinghe et al. (2006) indicated several shortcomings. The most obvious shortcoming of the predictive empirical relationship proposed by Black and Andrews (2001) is that erosion is not predicted to occur for any combination of obstacle dimensions.

Within a broader research program on coastal erosion funded by the Sardinian government, the University of Cagliari (Sardinia, Italy) has been acquiring data at different levels of detail and accuracy (using new field survey technology such as the Real-Time Kinematic Global Positioning System(RTK-GPS), and an image-derived survey method based on aerial and IKONOS satellite imagery) from the main salients along the coastlines of Sardinia, the second largest island of the Mediterranean Sea. We are not aware of any prior extensive survey of these morphologies in the

Mediterranean Sea and the paper presents the first database that maps the main properties of salient geometry and processes affecting their evolution. The objectives of this paper are to verify the equilibrium condition of shoreline behind natural emergent and submerged natural obstacles using the proposed semi-probabilistic method based on rate-of-change statistics, and to propose and validate predictive formulas for geometric properties of salients in equilibrium conditions along the Sardinian coastline, that overcome some limitations affecting previous works. By investigating the characteristics of natural obstacles and associated shoreline salients in Sardinia, the paper aims to provide practical insight into shoreline responses to engineered submerged structures that could be of value for coastal engineers and managers operating in the Mediterranean Sea where the wave climate and tide differ significantly from ocean conditions.

The paper is structured as follows. First, it summarizes field and image-derived surveys. Secondly, the shoreline analysis applied to a time series of digital shoreline position data is presented. In the framework of a semi-probabilistic model for shoreline change, two criteria are used to ascertain whether the salient has reached its equilibrium condition. Then, the paper extensively describes the model through its application to a salient located at Maladroxia beach (southwestern Sardinia). The next section summarizes the analysis of the equilibrium conditions of all selected salients along the Sardinian coastline. The results of these investigations on the development of a predictive relationship for shoreline response to natural obstacles are

discussed. Finally, specific knowledge gaps that require further research are identified in the conclusions.

STUDY SITE AND DATA DESCRIPTION

Sardinia is the second biggest island in the Mediterranean Sea. It has a wet season (October to April) accounting for 80% of the yearly precipitation with increasingly frequent heavy rainstorm events, and a dry season (May to September). The hydrographic service of the Italian Institute for Environmental Protection and Research (ISPRA) owns and manages the national networks of tide gauges (RMN) and data buoys (RON). Since 1986, RMN in Sardinian has been composed of three measuring stations with ultrasonic transducers located inside the harbors at Cagliari (south coast), Carloforte (southwest coast) and Porto Torres (north coast) (Fig. 1). Tide data reveals that the area is a microtidal coast with small differences between the three gauges. The data show astronomical mean spring and neap tide a range over the period 1988-2013 of approximately 0.30 m and 0.15 m, respectively, and an extreme storm surge value of approximately 0.50 m, with a return period of 100 years. Three Triaxys wave buoys have been deployed offshore from the Sardinian coasts to collect wave data continuously and provide synthetic and spectral parameters (Fig. 1). With the exception of the Alghero buoy (northwest coast) that covers the period between 1989 and 2008, data from the Cagliari and Capo Comino buoys (northeast coast) are not statistically significant. When not available from the RON dataset, data extracted from the "Wind and Waves Atlas of the Mediterranean Sea" (MEDATLAS,2004) and the Institute of Marine

Sciences of the Italian National Research Council (ISMAR-CNR) study (ISMAR-CNR, 2004) were used in this study. The Atlas contains bivariate tables of annual and seasonal frequency distributions of wave data (significant wave heights versus mean direction or peak period) resulting from a 10-yearhindcast based on a WAM model simulation calibrated with satellite altimeter measurements over a grid with a resolution of 1degree. In the case of the ISMAR-CNR wave dataset, a specific implementation of the WAM model was run at the ISMAR-CNR using the wind analysis and forecast fields from the European Centre for Medium-range Weather Forecast (ECMWF) as forcings with different meteorological model resolutions whose outputs were compared with altimeter and buoy data (Cavaleri and Bertotti, 2003). A Peaks-Over-Threshold time series was provided for 10 years over 6-hour intervals. The ISMAR-CNR wave dataset was used for beaches along the south coast. Fig. 1 shows the points along the Sardinian coasts considered in this study.

The geology along the Sardinian coastline varies, including both rocky coasts and low-lying sandy beaches. Most Sardinian beaches are remnants of the large sandy shoreline formed during the last glacial stage (Manca et al., 2013). At that time, lower sea levels resulted in erosion that uncovered the marine shelf sediments, which were then blown landward to form the main coastal dune systems and sandy deposits that characterize the western coast of Sardinia. The beaches are at risk of coastal flooding and erosion (Ginesu et al., 2016). Using digitized shorelines extracted from 1:25000 scale maps and aerial photographs, a recent report indicated that 14% of the

beaches have retreated at least 25 m in the past 50 years (ISPRA, 2010). Dunes are an important feature of Sardinia's coastlines and are usually fronted by wide sand beaches. Approximately 500 km of plains near the coastline are occupied by Quaternary deposits, principally aeolian sands. Being mostly relict features, the equilibrium of aeolian deposits is very sensitive to both climatic and anthropogenic factors (French et al., 1995). In the1960s, a phanerophyte native to Australia was introduced mainly in the coastal areas in Sardinia for afforestation. Currently, this area is considered naturalized, having become invasive in dunal habitats. *Posidonia oceanica* is a marine phanerogam endemic to the Mediterranean basin, which forms extended meadows along the Sardinian coast at a maximum depth of 30–40 m in clear water (Pergent et al., 1995). Dead leaves are frequently thrown up on beaches, especially during winter, forming banquettes that partially protect beaches from erosion (Jeudy de Grissac, 1984). Meadow regression may involve increases in energy and seabed slopethatalter shore profiles (Jeudy de Grissac and Boudouresque, 1985). Studies have been conducted to measure wave attenuation, transmission and energy dissipation in shallow waters over artificial *P. oceanica* meadowsin wave flumes in large-scale experiments (Infantes et al., 2009) and in the field (Infantes et al., 2012).

Study framework of Sardinian salients

Regardless of the degree of emergence or submergence, a large number of natural offshore obstacles (submerged reefs or islands) along Sardinia's coastlines interact with the coastal hydrodynamics and sediment transport processes. This interaction has resulted in changes in coastal morphology,

creating salients or tombolos in the lee of the obstacles. Since 2008, DICAAR has been carrying out a field- and imagery-derived survey to define a comprehensive database of these singular landforms. Individual landforms have been described in previous studies (Atzeni and Sulis, 2008; 2009a; 2009b; Sulis and Annis, 2014). Specifically, the wet/dry line (Leatherman, 2003) was used to identify the shoreline position and was derived from 3 different sources: cloudless orthorectified aerial photographs, satellite IKONOS multispectral images (European Space Imaging GmbH – Planetek Italia), and topographical surveys using RTK-GPS. Strengths and limitations of these data sources have been discussed in Sulis and Annis (2014).

This study focuses on salients. Specifically, 13 salients occur on the Sardinian coasts (Fig. 1). Salients are well spread along the entire coastof the island, thus being exposed to different wave and wind climates. Salients were treated as shoreline adjustments to the natural offshore obstacles, both emergent (islands) and submerged (reefs), superimposed to the existing natural shorelines. Fig. 2 shows how the smooth departures of salients from the undisturbed shorelines were identified in the case of a long straight beach (a), and a bay beach with single (b) and double (c) curvature. Each undisturbed shoreline examined in the present work belongs to the one of the above three cases.

We considered each offshore obstacle and the salient growth in its lee as morphological features. The analysis of geometric properties of the morphological features along Sardinia's coastline has required the adoption

of standard, non-ambiguous, definitions (Black and Andrews, 2001; Atzeni and Sulis, 2009a) as follows:

- *Baseline*: the line passing through the deepest point of the undisturbed curved shoreline on either side of the beach;
- *Shore normal*: the line passing through the salient apex, perpendicular to the baseline;
- *Length of the obstacle (B)*: the length equal to projection of the obstacle onto the baseline;
- *Width of the obstacle (W):* the distance at the widest part of the obstacle measured between the two tangents to the obstacle parallel to the baseline, nearest to and furthest from the latter;
- *Salient amplitude (Y):* the shore width between the baseline and the salient apex, perpendicular to the baseline;
- *Offshore distance of the obstacle (S):* the distance between the baseline and the nearest point of the obstacle, perpendicular to the baseline;
- *Salient basal width (D):* the total length of shoreline affected.

These properties are presented for the Maladroxia salient in Fig. 3. All values of geometrical properties in the 13 salients result from more recent topographical surveys using RTK-GPS that have an assured high level of accuracy (within 1.2 cm planimetrically). The measured values of the different variables mainly involved in the salient geometry (B, W, Y, S, D, B/S) are given in Table 1. The distance of the two diffraction points (P_L and P_R) is also reported in Table 1. As expected, all the measurements in Table 1

reveal a high variability in field observations that reproduce a large number of favorable conditions for salient growth in the lees of natural offshore obstacles. It is worth noting that previous analysis on geometrical properties of these morphological features (e.g., empirical relationship to predict salient amplitude or non-dimensional ratio to control coastal morphology) have considered the distance S as one of the governing parameter regardless the distance P that takes into account the effect of diffraction. This could be justified by the fact that previous studies have mainly focused on single or multiple emergent breakwaters where S and Pare mainly coincident, being the diffraction (or control) point located in the landward corner of the breakwater as reported in the extensive dataset of Hsu and Silvester (1990). In the case of complex natural obstacles, both emergent and submerged, S and P could be significantly different in value and their practical utility. While S is mainly used to identify the distance of the natural obstacle from the baseline (Black and Andrews, 2001), P is a part of the coordinate system of some static equilibrium-shaped models (Hsu et al., 2010). In the case of complex irregular obstacles there are some difficulties in locating the diffraction point (Gonzáles and Medina, 2001). In this paper, the parabolic bay shape model (Hsu et al., 2010) was applied in a trial-and-error procedure to find the L value that gives a predicted shoreline almost identical to the existing shoreline considered in equilibrium condition (see below).

At all 13 selected beaches, surface sediment samples were collected at the same time that the shoreline positions were surveyed. A sampling scheme

was developed to adequately sample the beaches in the alongshore directions specifically related to morphology zones and shoreline variability. Each sample consisted of approximately 300 g. Beach sediments are predominately quartzose; only Maladroxia and Tuarredda have sediments that are compositionally bimodal with admixtures of biogenic carbonate fragments and silicate grains. Samples were sieved with demineralized water through a 4ϕ sieve to separate the mud fractions; then, sand grain size analysis was performed by dry sieving at ½ϕ intervals. Statistical parameters of grain size distributions were obtained using the moments method according to Folk (1974). Grain size is fairly constant alongshore, a likely occurrence on small beaches with significant alongshore sediment transport - the latter being an intuitive condition for shoreline accretion in the lees of offshore obstacles (Ranasinghe et al., 2006). For each beach, the average values of sediment median and sorting are reported in Table 2; these values represent the most important grain size parameters in our study. Beaches showed highly variable grain sizes, from fine sand at Maladroxia (2.178 ϕ) to very coarse sand at Tinnari (-0.456 ϕ), while the sorting degree of the sand samples ranged from very well sorted at Tinnari (0.152 ϕ) to moderately sorted at Vignola (0.568 ϕ). No salients consisted of poorly sorted sand, as expected in the lees of obstacles that dissipate the energy of incident waves.

The longshore component of the wave energy flux per unit of length of the 13 beaches was computed using the approximated formula of Galvin and Schweppe (1980) (cf. Atzeni, 2011):

$$P_{lbs} = \frac{\pi K_s^3}{8k} \rho g \frac{\left(\sqrt{e} H_{0S}\right)^3}{T_S} \sqrt{|cos\alpha_0|} sin2\alpha_0 \quad (1)$$

whereH_{0s}, α_0 and T_S are the height, the angle between the normal to the wave mean direction and the shoreline (Table 2 reports the normal direction, α_n), and the period of the significant wave at the nearest deepwater point of the wave database, respectively. K_S is the shoaling coefficient (K_S= 0.7 at the breaker), k is the breaker index, and e is the wave energy ratio (a Mitsuyasu-type directional spreading function with spreading parameter s_{max} = 10).

Sensitivity analysis of magnitude and direction along the west coast of Sardinia was investigated by Sulis and Annis (2014). The magnitudes of time-averaged longshore flux are reported in Table 2, along with the dominant wave directions α_{dom} according to Gonzales and Medina (2001). The magnitudes are clearly related to the different wave climates along the Sardinian coast, with the northwest area of the island being the most energetic in the Mediterranean Sea. Magnitudes were found to range between 37 W/m at Maladroxia in the inner Golf of Palmas to 2473 W/m at Lu Bagnu in the northern coast, which is particularly subjected to direct storms in the offshore Gulf of Lyon (France).

SHORELINE ANALYSIS

The response of shoreline changes behind natural obstacles is an exceedingly slow process, and thus criteriahave been applied to ascertain whether the shoreline in the lee of an offshore obstacle has reached its equilibrium condition. To assure a common analysis for a wide range of

shoreline features, this paper proposes the following 5-step approach that has been applied to the 13 beaches where salients occur:

1. Beach survey and acquisition of aerial and IKONOS satellite imagery;
2. Shoreline mapping process (manual);
3. Compilation and editing of time series of digital shoreline position data in the ESRI ArcGIS environment;
4. Digital shoreline analysis using the Digital Shoreline Analysis System (DSAS);
5. Probabilistic model for shoreline change.

As shorelines are derived from various sources such as aerial photographs, satellite images and field GPS surveys, the wet/dry line was selected as a common indicator to allow for comparison of positional changes through time (Zhang et al., 2002; Leatherman, 2003). Wet/dry lines were manually depicted on cloudless orthorectified aerial photographs from 1954, 1968, 1997, 2000, 2003, 2004, 2006 and 2008 (pixel sizes between 0.20 and 1 m), satellite IKONOS multispectral images from 2005 (pixel sizes of 0.8 m), and GPS measurements with permanent RTK (Real-Time Kinematic) corrections from station data from 2009 to 2011 (accuracy within 2 cm) (Table 3). Digitized shorelines were represented in a geographic information system (GIS) platform (ArcGIS 10.1; EsriSoftware). DSAS (Thieler et al., 2009) calculates shoreline rates of change from the time series of shoreline position data.

The DSAS programs extend the functionality of the ArcView GIS software to include historic shoreline change analysis.

The main features of DSAS allow users to:

- define a landward baseline, comprisingmultiple lines that may not be totally straight, each of which should be entirely seaward or landward of the shorelines;
- generate orthogonal transects at the user-specified interval;
- calculate the rate-of-change statistics.

DSAS employs a measurement baseline approach to simultaneously calculate the rate-of-change statistics. Fig. 4 shows the application of this approach to Maladroxia beach, where a landward baseline and 41 transects were defined in the central part. Among numerous standard methods for shoreline analysis reviewed by Dolan et al. (1991), the latest version of DSAS calculates the Net Shoreline Movement (NSM), the Shoreline Change Envelope (SCE), the End-Point Rate (EPR), and the Linear Regression Rate, either simple (LRR) or Weighted (WLR), at user-specified intervals along the shoreline. Thieler et al. (2009) provides an in-depth presentation of these methods. The SCE and the NSM report distances, not rates, between the shorelines farthest from and closest to the baseline and between the oldest and the youngest shoreline, respectively, at each transect, and thus are not useful in this analysis. In contrast, the EPR is calculated by dividing the NSM by the time between the oldest and the youngest

shoreline. The major disadvantage of the EPR is that it neglects the information from additional available shorelines, missing changes in sign (accretion versus erosion) or magnitude of the shoreline movement trend, or cyclicity of the shoreline behavior. In the case of shoreline positions, Linear Regression (LR) reveals a relationship between position and time. While some limitations of the linear model in reproducing the complex relationship between time and shoreline position have been highlighted by several authors (Dolan et al., 1991; Fenster et al., 1993), Zhang et al. (2002) indicate that more complex models can result in highly inaccurate predictions. In this study, it is assumed that a linear model is adequate for modeling long-term shoreline evolution in the lee of the natural obstacle (primary evolution). The LR was obtained by fitting a least-squares regression line to all shoreline points along a user-selected transect. The LRR is the slope of the regression line, corresponding to the amount of regression or accretion per year. Moreover, the coefficient of determination (R^2) was computed to reveal what fraction of the variance of the shoreline position is attributable to time. Using the available shoreline positions, the model is:

$$y(t) = a_1 + a_2 t + \varepsilon \tag{2}$$

where t is the time, y is the shoreline position and ε is its random deviation, a_1 and a_2 are the estimates of the y-intercept and the line slope (LRR value), respectively.

Here, the probabilistic model of shoreline change proposed by Douglass et al. (1999) is adopted. In this model (2), any historical shoreline position includes a random component due to recently experienced waves superimposed on a long-term signal modeled as a linear function of time. A significant number of shoreline positions over time is needed to make evident the long-term primary response, in spite of random fluctuations. Several fundamental parameters (Dolan et al., 1980) can be used to test the validity of the application of adopted rates, EPR and LRR. In this study, two main approaches were tested, namely, the signal to noise (S/N) ratio (Thieler and Danforth, 1994) for EPR and the Confidence Interval (CI) technique (Douglass et al., 1999) for LRR.

To compute the S/N ratio, the Maximum Expected Error (MEE) in the position of a wet/dry line at time *t* was calculated. When considering the oldest (*t=t1 years*) and the youngest (*t=t2 years*) lines as independent observations, the S/N ratio is:

$$(S/N) = \frac{MEE_{t1} + MEE_{t2}}{t2 - t1} \tag{3}$$

Considering the *j-th* profile, the EPR_j is considered not detectable if:

$$\left|EPR_j\right| \leq (S/N) \tag{4}$$

This approach is deterministic. Whereas the accuracy and precision of the survey method can be quantified, the wet/dry position is considerably affected by several sources of uncertainty (essentially, water level

fluctuations due to tides, winds, barometric pressure and waves; for instance, see Morton and Speed, 1998).A thorough statistical analysis is beyond the scope of this paper. To be conservative, Douglas and Crowell (2000) suggest adding to the MEE a random component of uncertainty equal to a site-specific fraction of beach width (20% in their study). We preferred to significantly reduce the main sources of uncertainty with a proper selection of data at each site. When estimating those sources of uncertainty, the Total Maximum Expected Error (TMEE = MEE + uncertainty) must be used in Eq. (2).

The linear portion of Equation (2) provides an estimate of the mean wet/dry line position. The CI technique can provide useful information on the reliability of such an estimate, particularly regarding the slope (a_2 in Eq. 2). The confidence interval (δ) provides an estimated range Z=[a_2-δ/2, a_2+δ/2] for the trend to include, with a user-defined probability (level of confidence), the true long-term primary evolution. The no-trend condition at *j-th* profile is given as:

$$0 \in \left[a_2 - \delta/2, a_2 + \delta/2 \right] \tag{5}$$

wherein the range *Z* of shoreline trend includes zero shoreline change and there is no evidence of long-term primary evolution. The selection of the proper level of confidence is a crucial aspect of the proposed approach, as reducing the desired confidence level will result in fewer salients with the no-trend condition. Because salient evolution analyses based on a few historical shoreline positions have degrees of freedom such that the

confidence intervals are extremely wide, these analyses will likely include the no-trend condition in the primary responses of salients. In the absence of a priori information on data uncertainty, a range Z at a 95% confidence level was selected herein (Douglas and Crowell, 2000).

We suggest a value of 80% of the beach length, or 80% of the transect number where conditions (4) and (5) are satisfied, as the threshold above which the *EPR* is considered to be undetectable and there is no evidence of long-term primary evolution on the beach; hence, the entire beach and the included salient is considered to be at equilibrium. As the verifications of conditions (4) and (5) require different amounts of information at different levels of accuracy, it is suggested that condition (4) should be considered first; only if the *EPR* can be considered detectable based on the potential maximum error estimation on shorelines positions, should the more complex issue of whether erosion was taking place at the 95% level of confidence be analyzed by checking condition (5).

RESULTS AND DISCUSSION

Shoreline equilibrium analysis at Maladroxia beach

Fig. 4 presents the application of DSAS to Maladroxia beach (38°59’56’’N, 8°26’56’’E), located in the east coast of Sant’Antioco Island, southwest of Sardinia. Maladroxia is a pocket beach extending for approximately 400 m between two rocky headlands and is characterized in its central part by a salient shape due to a submerged reef of an area of approximately 1 hectare and location 45 m seaward from the undisturbed shoreline (Table 1). The

beach sediment comprises rather moderately well-sorted, fine-grainedsands. The dominant wave direction (as inGonzales and Medina, 2001) from deep-water waves obtained by ISMAR-CNR (2004) model is 151°N (Table 2).Using the simplified approach proposed by Sulis and Annis (2014), the estimated time-averaged longshore flux reaches a value of up to 37 kW/m. The input data for the DSAS analysis consisted of 12 shoreline positions from eight color or black and white cloudless orthorectified aerial photographs (1954, 1968, 1977, 2000, 2003, 2004, 2006 and 2008), one IKONOS multispectral satellite image (2005), and three topographical surveys using RTK-GPS (2009, 2010, 2011) (N_{yy}=12). Data available for the example of Maladroxia do not include extreme shoreline positions, and come from the same period where low energy was expected. These data are representative of all salients in Sardinia where the expected positional accuracy is good in relation to the rate of shoreline change that needs to be measured, and the inherent errors that need to be quantified. Specifically, the magnitude of the digitizing errors (random error) was minimized by testing the repeatability of measurements. Here, the more conservative estimate of MEE in the position of the oldest (*t1=1954*,from aerial photographs) and youngest (*t2=2011*,from RTK-GPS surveys) lines was equal to 10 m and 0.5 m, respectively. Special care was taken in selecting these two records (same period with low energy, calm sea surface) and an approximate and conservative estimate of sea-level variations due to tides gives a value of uncertainty in the wet/dry line position of 2 m. We obtained $TMEE_{j,1954}$= 12.0 m and $TMEE_{j,2011}$= 2.5 m.

In the DSAS graphical interface, we defined the measurement baseline as a single line tangent representing the undisturbed curve shoreline at its deepest point on both sides, and 41 transects with 4 m-intervals were automatically generated according to the user-specified parameters (Fig. 4). No manual corrections were required to avoid transect intersections. Fig. 5 shows that the EPR is within the S/N limits, equal to ±0.254 m/yr (erosion vs accretional dominated shoreline trends) along 39 out of 41 of the salient transects. Here, the S/N ratio exceeds the EPR value along more than 95% of the salient length (Y).

Fig. 6a shows shoreline position data available during the period 1954-2011 along the transect passing through the salient apex. The LRR value is equal to 0.03 m/yr, and the CI for a level of confidence of 95% gives δ=0.15. The estimated range Z=[-0.045, 0.105] includes the zero shoreline change, and there is no evidence of a trend along this profile. Considering all 41 profiles, 80% of the salient length fulfills the no-trend condition (5) at the same level of confidence. Notably, however, approximately 20% of the salient length shows a linear trend evolution. Fig. 6b shows the shoreline position during the period 1954-2011 along transect number 5 (see Fig. 4: transects are numbered from the south), revealing a linear trend condition with LRR = -0.17 m/yr and δ=0.10 (at a confidence level of 95%). In this transect, the standard deviation of measurement residuals r (~ 0.75 m) is significantly lower than the minimum *TMEE* of the available database ($TMEE_{j,2011}$= 2.5 m), reflecting the appropriateness of the adopted LR model.

According to the data resolution, more than 80% of the salient at Maladroxia beach fulfills both conditions (4) and (5) for the S/N and CI methods to determine the validity of EPR and LRR, respectively. These results suggest that the long-term primary evolution at Maladroxia cannot be considered detectable and that the salient can be considered to be in equilibrium.

Overview of Sardinian shoreline equilibrium analysis

The proposed approach was used for the 13 salients at the Sardinian coasts following the procedure presented above in the application to Maladroxia beach. Seven salients are in the lees of emergent obstacles, while 6 salients are behind submerged reefs. Each feature was classified into three different types: pocket beach salient, symmetrical salient, and asymmetrical salient. Notably, in the pocket beach cases, salients may not be significantly affected by adjacent rocky headlands. Additionally, the symmetry is of planimetrical type in relation to the shore-normal line without considering the dominant wave direction. Based on the more recent RTK-GPS topographical surveys, 4 salients were classified as symmetric, 4 as asymmetric, and 5 as pocket beach salients. Whereas aerial photographs and IKONOS images cover all the Sardinian coasts, cloud or storm-influenced data were excluded from the DSAS application to a single beach. From 2009 to 2011, GPS measurements were conducted at different frequencies.

The selected number of data points (N_{yy}) used for shoreline extraction at different beaches is summarized in Table 4. Given that the oldest imagery

available (*t=t1 years*) is beach-dependent, the more conservative estimates of MEE_{t1} and $TMEE_{t1}$ show significant variability among different salients; consequently, the beaches are characterized by different values of S/N. Based on the occurrence of secondary morphological features, a user-specified number of transects N_t with a constant distance d were considered in the DSAS to calculate EPR and LRR values. Table 4 summarizes for each beach the percentages of transects where the EPR is within the S/N limits and the range Z for a level of confidence of 95% that includes the zero shoreline change. Twelve out of 13 salients satisfy both conditions (4) and (5) at more than 80% of the beach transects and can thus be considered to be in equilibrium. The salient at Capo Comino fulfills the no-trend condition at 60% of the selected transects, providing evidence of the long-term primary evolution of this morphology.

Salient geometrical properties

In the framework of the standard definitions of salient geometrical properties, the values of the 12 features with salients in equilibrium are reported in Table 1. The alternative distance X (X=S-Y) is also reported. Values were extracted using the most recent available shorelines. The process of sand deposition in the lee of a natural offshore obstacle depends on several parameters, including wave parameters, beach sediment characteristics, bathymetry data, and others. Numerous studies have emphasized that the B/S ratio fundamentally controls coastal morphology

both behind artificial structures such as breakwaters (Nir, 1982; USACE, 1984) and natural obstacles (Black and Andrews, 2001), whereas other parameters are of secondary importance. A correlation analysis between the (S-Y)/B ratio and the B/S ratio, shoreface slope *s* (data from Di Gregorio et al., 2000), longshore component of the wave energy flux P_{lbs} (Sulis and Annis, 2014) and median grain size D_{50} has substantiated these findings with a Pearson correlation coefficient ρ equal to 0.48, 0.34, 0.145 and 0.06, respectively. The dimensionless variable B/S is reported in Table 1; it is adopted as the salient limiting parameter for reefs and islands. Some investigations have highlighted that the characteristics and processes governing long-term primary evolution in the lees of submerged and emergent offshore obstacles are fundamentally different (Ranasinghe and Turner, 2006). In particular, to account for the effects of wave transmission on limiting parameters in this work, data from submerged reefs and islands were considered separately. According to Black and Andrews (2001), the data indicate that all four salients behind islands occur with variable B/S ratios lower than or equal to 1, similar to emergent breakwater B/S ratios (Silvester and Hsu, 1997). Two data points from salients behind submerged reefs significantly fall beyond the B/S ratio of 2 suggested by Black and Andrews (2001). Specifically, the features at Maladroxia and Platamona show B/S ratios equal to 3.93 and 3.10, respectively. However, data from offshore reefs in the Black and Andrews(2001)study suggest that only tombolo formation occurs at B/S ratios higher than 2. Several shortcomings in the methodology adopted by Black and Andrews could partially explain this inconsistency. In particular, a quantification of shape and dimensions of

complex natural reefs by visual inspection of low accuracy aerial photographs in the absence of field surveys may have affected the accuracy of the results of this unique study. The results at Maladroxia and Platamona suggest that site-specific wave transmission in the lees of offshore reefs allows a broader range of salient limiting B/S ratios. The portion of wave energy that passes over the submerged obstacle depends on the reef width (W) and average submergence depth (d_s), similar to freeboard and crest width affecting the wave transmission over a submerged breakwater (Seelig, 1980). The reef at Maladroxia has a $1\text{-}d_s/d$ ratio (d: the water depth at the offshore limit of the reef) approximately equal to 0.1, whereas the W/L_{rep} ratio (L_{rep}: representative wave length as defined by Sulis and Annis, 2014) at Platamona is approximately equal to 0.25. Both the $1\text{-}d_s/d$ and W/L_{rep} ratios are significantly lower than in other examined salients. Higher ratios are expected to determine a reduction of the wave energy reaching Maladroxia and Platamona beaches to a higher degree compared to other sites, and this could partially explain the formation of salients instead of tombolos as predicted by previous limiting parameters.

Previous approaches used scattered data to determine an empirical relationship that predicts salient amplitude from non-dimensional variables (Rosen and Vajda, 1982). Hsu and Silvester (1990) showed that when (S-Y)/B is plotted against B/S, a single curve exists in the case of a single breakwater parallel to the coast with normally incident waves. Considering 14 salients not affected by adjacent headlands, Black and Andrews(2001)identified two power-curve relationships from island and

natural reef data. These empirical relationships are shown in Fig. 7 for comparison. As reported by Ranasinghe and Turner (2006), findings from this comparison are counterintuitive as it appears that a submerged obstacle would result in a larger salient in its lee than one that would result from an emergent breakwater of equal size located in exactly the same offshore location. In Fig. 7 the ratio (S-Y)/B is plotted against B/S for the entire database of 12 salients in the lees of natural reefs and islands along the Sardinia coastline. Data on salients for islands and natural submerged reefs exhibit similar power-curve relationships. For B/S<0.7, the island curve predicts salient amplitude values slightly higher than submerged reefs, whereas for B/S>0.7, differences between predicted reef and island values are always lower than 0.03. As these differences are considered negligible compared with the data of TMEE in the entire range of practical use of prediction curves, the following power-curve relationship was defined for reef and island data combined:

$$\frac{S-Y}{B} = 0.48\left(\frac{B}{S}\right)^{-1.23} \tag{6}$$

An adjusted coefficient of determination R^2= 0.80 demonstrates the goodness of fit data for the proposed model (Fig. 8). The salient amplitude values are considered here as random variables, and the reliability of predicted values is estimated by providing prediction intervals. Prediction intervals are also shown in Fig. 8 and give an indication of how likely it is that a salient observation will fall within the interval around the expected value given by Eq. (6). The model prediction accuracy is quantified by

using the 95% prediction interval. Notably, both reef and island values predicted by Black and Andrews(2001) fall within the prediction intervals at 95%.

Sunamura and Mizuno (1987) and Black and Andrews (2001) presented empirical relationships that predict salient width from non-dimensional variables. Both results suggested that Y/D is independent from other non-dimensional variables, and D is approximately eight times Y. However, these analyses were affected by data scattering. Moreover, a high level of uncertainty was expected in Black and Andrews' measurements from aerial photographs of the actual length of a feature that is asymptotic to the original shoreline. The ratio Y/D is plotted against S/B in Fig. 9 for the entire database of the 12 stable salients along the Sardinian coastline, together with data provided by Black and Andrews (2001). Fig. 9 shows that the scatter does not permit any suitable relationship, including the '8 times rule', to be derived. To non-dimensionalize D and S, we choose B as the common variable. When the ratio D/B is plotted against B/S, as shown in Fig. 10, a curve-fitting analysis yields the power-curve relationship:

$$\frac{D}{B} = 2.95\left(\frac{B}{S}\right)^{-0.83} \tag{7}$$

with an adjusted coefficient of determination R^2= 0.84. More complex analyses do not produce better curve fitting performance, at least for salients along the Sardinian coastline. The reliability of predicted width values is quantified by using the 95% prediction interval. Confidence intervals are

more informative than the simple relationship indicated by Equation 7,because Fig. 10 provides a range of plausible values for salient width, and the extension of that range can give us some idea about how uncertain we are about the estimation of this geometrical property of the salient. For a value of B/S =1.5, D/B = 2.1 ± 50%, while wider intervals correspond to higher B/S values. For example, for B/S =2.6, the interval is twice the predicted D/B value. Very large intervals for higher B/S values indicate that the level of uncertainty associated with Equation 6 does not allow for the proper prediction of salient width, and more data should be collected to achieve a narrower interval and more precise width prediction in a salient with a high B/S value.

CONCLUSIONS

This paper proposes geometric predictive formulas for salient morphological features that overcome some limitations affecting previous works. A semi-probabilistic method based on well-known rate-of-change statistics is also presented to verify the equilibrium condition of salients. Analyses and tests were performed considering salients in the lee of natural obstacles, both submerged reefs and islands, spread along the Sardinia's (Italy) coastlines exposed to different wave and wind climates. In our knowledge this is the first attempt to define empirical relationships for the morphology of natural salients and their geometries in the Mediterranean sea, as previous main works have focused on oceanic beaches. Also, the levels of detail and accuracy of field survey of the Sardinia salients through RTK-GPS, significantly differ from previous studies of researchers that

visually inspected low-resolution aerial photographs. While analysisresults confirm that the main variables in evaluating salient geometric properties are the length of the obstacle (B) and the distance between undisturbed beach and obstacle (S), it is suggested that site specific wave transmission in the lee of submerged reefs requires a range of salient limiting B/S ratio values broader than those presented in the literature. In the case of natural salients in the lee of submerged reefs,the width and average submergence depth of reef could also be of value as parameter affecting the shoreline response when the crest is shallower and wider. The B/S ratio has been proved to be the main dimensionless variable to predict the salient amplitude (Y) and basal width (D). The proposed predictive equation suggests erosion condition for some combination of B/S overcoming the most obvious shortcoming of the Black and Andrews' (2001) predictive empirical relationship by which erosion is not predicted to occur for any combination of obstacle dimensions:

$$\frac{S-Y}{B} = 0.48\left(\frac{B}{S}\right)^{-1.23}$$

In addition, the "8 times rule" for salient width (Sunamura and Mizuno, 1987) does not appear to be applicable to natural salients and the following predictive equation has been proposed:

$$\frac{D}{B} = 2.95\left(\frac{B}{S}\right)^{-0.83}$$

However, very large 95% confidence intervals for higher B/S values indicated that the level of uncertainty associated with this equation does not allow us to properly predict salient width, and data from salients in other countries along the Mediterranean sea could improve the quality of the prediction.

The increasing amount of field- and imagery-derived survey products (cloudless orthorectified aerial photographs, satellite IKONOS multispectral images, and digital elevation models from RTK-GPS or drone) now allows for a broader applicability of the proposed semi-probabilistic method to other beaches in terms of engineering design, operations and maintenance issues. The semi-probabilistic model uses LR to reveal a relationship between position shoreline and time along a user-selected transect. LR uses no physical knowledge and extracts the relations that describe the properties of data from the data itself. Although LR is based on the internal structures found in the field- and imagery-derived survey products, a multi-variate probabilistic model (e.g. Dong and Chen, 1999) should be used when it is important to understand the nature of underlying processes and how these processes are reflected in the long-term shoreline evolution in the lee of the natural obstacle.

ACKNOWLEDGEMENTS

This work was partially funded by the Sardinian government (RAS) under the P.O.R. Sardegna F.S.E. Operational Programme of the Autonomous

Region of Sardinia, European Social Fund 2007-2013—Axis IVHuman Resources, Objective 1.3, Line of Activity I.3.1.

REFERENCES

Atzeni,A., 2011. Dispense di Idraulica Marittima. Aracne Editrice, Rome,(in Italian), 400 pp.

Atzeni, A., and Sulis, A., 2008. Morphological impact of submerged natural reef along Is Morus, Sardinia: insight and preliminary results. Proceedings of the 9th International Conference LITTORAL 2008, Venice, Italy.

Atzeni, A., and Sulis, A., 2009a. Morphology of the salient of Su Giudeu beach (Sardinia, Italy) and hydrodynamic along the shoreline. Proceedings of the 4th SCACR – International Conference on Applied Coastal Research, Barcelona, Spain.

Atzeni, A., and Sulis, A., 2009b. Morphology of the salient of Tuerredda beach (Sardinia, Italy) and hydrodynamic along the shoreline. Proceedings of the 9th International Conference on the Mediterranean Coastal Environment MEDCOAST 09, Sochi, Russia.

Black, K.P., and Andrews, C.J., 2001. Sandy shoreline response to offshore obstacles. Part 1: Salient and tombolo geometry. Journal of Coastal Research, SI 29, 82-93.

CNR-ISMAR, 2004. Ricostruzione del climaondoso al largo di Cagliari. ISMAR-CNR Technical Report (in Italian), 35 pp.

Cavaleri, L. and Bertotti, L. 2003. The characteristics of wind and wave fields modelled with different resolutions. Q.J.R.Meteorolog.Soc., 129, 1647-1662.

Damgaard, J., Dodd, N., Hall, L. andChesher, T., 2002. Morphodynamic modelling of rip channel growth. Coastal Engineering, 45, 199-221.

Danish Hydraulic Institute — DHI, 2008. MIKE 21, Release 2008, User Guide and Scientific Documentation.

Di Gregorio, F., Federici, P.R., Fierro, G., and Ginesu, S., 2000. Atlante delle Coste della Sardegna. Regione Autonoma della Sardegna, CNR and MURST.

Dolan, R., Fenster, M.S. and Holme, S.J., 1991. Temporal analysis of shoreline recession and accretion. Journal of Coastal Research, 7(3), 723-744.

Dolan, R., Hayden, B.P. May, P., and May S., 1080. The reliability of shoreline change measurements from aerial photographs. Shore and Beach, 48, 22-29.

Dong, P., and Chen, H., 1999. A probability method for predicting time-dependent long-term shoreline evolution. Coastal Engineering, 36(3), 243-261.

Douglas, B.C., and Crowell, M., 2000. Long-term shoreline position and error propagation. Journal of Coastal Research, 16(1), 145-152.

Douglass, S.L., Sanchez, T.A., and Jenkins, S., 1999. Mapping erosion hazard areas in Baldwin County, Alabama and use of confidence intervals in shoreline change analysis. Journal of Coastal Research, SI 28, 95-105.

Fenster, M.S., Dolan, R., and Elder, J.F., 1993. A new method for predicting shoreline positions for historical data. Journal of Coastal Research, 9(1), 147-171.

Folk, R.L., 1974. Petrology of Sedimentary Rock.Hemphill Publishing Company, Austin, TX.

French, J.R., Spencer, T. and Reed, D.J., 1995. Geomorphic response tosealevel rise: existing evidence and future impacts. Earth SurfaceProcesses and Landforms 20, 1-6.

Galvin, C.J., and Schweppe, C. R., 1980. The SPM energy flux method for predictinglongshore transport rate. Technical Paper 80-4, U.S. Army Engineer Waterways Experiment Station, Vicksburg, MS.

Ginesu, S:, Carboni, D., Marin, M., 2016. Erosion and use of the coast in the northern Sardinia (Italy). Procedia Environmental Sciences, 32, 230-243,

Gonzáles, M., and Medina, R., 2001. On the application of static equilibrium bay formations to natural and man-made beaches. Coastal Engineering, 43 (3-4), 209-225.

Hakeem, J., Wilkens, J., Parsons, A., and Chester, T., 2010. Modelling the effect of nearshore detached breakwaters on sandy macro-tidal coasts. Environment Agency report. Project: SC060026/R2, Bristol.

Hanson, H., and Kraus, N.C., 2011. Long-term evolution of a long-term evolution model. Journal of Coastal Research, SI (57), 118-129.

Hsu, J.C.R., and Evans, C., 1989. Parabolic bay shapes and applications. Inst. Civ. Eng., Proc., London, England 87, 556-570 (Part 2).

Hsu, J.C.R., and Silvester, R., 1990. Accretion behind single offshore breakwater. Journal of Waterway, Port, Coastal and Ocean Engineering, 116 (3), 367-380.

Hsu, J.R.C., Yu, M.J., Lee, F.C., and Benedet, L. , 2010. Static bay beach concept for scientists and engineers: A review. Coastal Engineering, Special Issue 57 (2), 76-91.

Hsu, T.W., Jan, C.D., and Wen, C.C., 2003. Modified McCormicks model for equilibrium shorelines behind a detached breakwater. Ocean Engineering, 30 (15), 887-897.

Infantes, E., Orfila, A.,Terrados, J.,Luhar, M.,Simarro, G. andNepf,H., 2012. Effect of a seagrass (Posidoniaoceanica) meadow on wave propagation. Mar. Ecol. Prog. Ser., 456, 63-72.

Infantes, E.,Terrados, J.,Orfila, A.,Cañellas, B. and Álvarez-Ellacuria, A., 2009. Wave energy and the upper depth limit distribution of Posidonia oceanica. Botanica Marina, 52, 419-427.

ISPRA, 2010. Annuario dei dati Ambientali. Edizione 2010. Istituto Superiore per la Protezione e la Ricerca Ambientale. In Italian. http://annuario.isprambiente.it/content/versioni

Jeudy de Grissac, A., 1984. Effects des herbiers à Posidoniao ceanica sur la dynamique marine et la sédimentologie littorale. In: C.F. Boudouresque, A. Jeudy de Grissac, J. Oliver (Eds.), International workshop on Posidoni aoceanica Meadows, Vol. 1GIS Posidonie, France, 437–443

Jeudy de Grissac, A. andBoudouresque, C.F.,1985. Rôles des herbiers de phanérogames marines dans les mouvements des sediments côtiers: les herbiers à Posidonia oceanica. Colloque franco-japonais Oceanographie. Marseille, 16–21 September 1985, 1, 143–151.

Kristensen, S.E., Drønen, N., Deigaard, R., and Fredsoe, J., 2013. Hydrid morphological modelling of shoreline response toa detached breakwater. Coastal Engineering, 71, 13-27.

Lamberti, A. and Zanuttigh, B. 2009. Low crested breakwaters. In: Kim, Y.C. (Ed.), Handbook of Coastal and Ocean Engineering,World Scientific, pp. 601-632.

Leatherman, S. P. 2003. Shoreline Change Mapping and Management Along the U.S. East Coast. Journal of Coastal Research, 38, 5–13.

Lesser,G.R., Roelvink, J.A., van Kester, J.A.T.M., Stelling, G.S., 2004. Development and validation of a three-dimensional morphological model. Journal of Coastal Engineering, 51, 883-915.

Manca, E., Pascucci, V., De Luca, M., Andreucci, S., 2013. Shoreline evolution related to coastal development of a managed beach in Alghero, Sardinia, Italy. Ocean & Coastal Management, 85, 65-76.

MEDATLAS Group, 2004. Wind and wave atlas for the Mediterranean Sea, Western European Union, WEAO Research Cell, pp 419.

Mei, C.C., 1983. The applied dynamics of ocean surface waves. World Scientific Publishing, Singapore.

Mory, M. and Hamm, L., 1997. Wave height, setup and currents along a detached breakwater submitted to regular or random wave forcing. Coastal Engineering, 31 (1-4), 77-96.

Morton, R.A. and Speed, F.M., 1998. Evaluation of shorelines and legal boundaries controlled by water levels on sandy beaches. Journal of Coastal Research, 14(4), 1373-1384.

Nir, Y., 1982. Offshore artificial structures and their influence on the Israel and Sinai Mediterranean beaches. 18th Coastal Eng. Conf., ASCE, Cape Town, Suth Africa, 1837-1856.

Pergent, G.,Pergent-Martini, C. and Boudouresque, C.F., 1995. Utilisation de l'herbier à Posidonia oceanica comme indicateur biologique de la qualité du milieu littoral en Méditerranée: état des connaissances. Mesogée, 54, 3–27.

Ranasinghe, R., and Turner, I.L., 2006. Shoreline response to submerged structures: a review. Coastal Engineering, 53, 65-79.

Ranasinghe, R., Turner, I.L., and Symonds, G., 2006. Shoreline response to multi-functional artificial surfing reefs: a numerical and physical modelling study. Coastal Engineering, 53, 589-611.

Roelvink, D., and Reniers, A., 2011. A Guide to Modelling Coastal Morphology, Advances in Coastal and Ocean Engineering, Volume 12, World Scientific Publishing, Singapore.

Rosen D.S., and Vajda, M., 1982. Sedimentological influence of detached breakwaters. Proceedings 18th International Conference on Coastal Engineering, ASCE, 1930-1949.

Seelig, W.N., 1980, Two-dimensional Tests of Wave Transmission and Reflection Characteristics of Laboratory Breakwaters, Tech. Rept. No. 80-1, US Army Coast. Engrg. Res. Ctr., Fort Belvoir, VA.

Silvester, R., and Hsu, J.C.R., 1997. Coastal stabilization. World Scientific Publishing, Singapore.

Sulis, A. and Annis, A. 2014. Morphological response of a sandy shoreline to a natural obstacle at Sa Mesa Longa Beach, Italy. Coastal Engineering, 84, 10-22.

Sunamura, T., and Mizuno, O., 1987. A study on depositional shorelines behind an island. Annual Report, 13, Institute of Geosciences, University of Tsukuba, 71-73.

Thieler, E.R., and Danforth, W.W., 1994. Historical shoreline mapping (II): Application of the Digital Shoreline Mapping and Analysis Systems

(DSMS/DSAS) to shoreline change mapping in Puerto Rico. Journal of Coastal Research, 10(3), 600-620.

Thieler, E.R., Himmelstoss, E.A., Zichichi, J.L., and Ergul, A., 2009. Digital Shoreline Analysis System (DSAS) version 4.0 — An ArcGIS extension for calculating shoreline change. U.S. Geological Survey Open-File Report 2008-1278.

U.S. Army Corps of Engineers, 1984. Shore Protection Manual 4th ed., U.S. Government Printing Office, Washington, D.C. (in 2 volumes).

Zhang, K., Huang, W., Douglas, B.C. and Leatherman, S.P., 2002. Shoreline position variability and long-term trend analysis. Shore and Beach,70(2), 31–35.

FIGURES

Fig. 1. Map of the island of Sardinia showing locations of the 13 salients, RON and RMN gauges and MedAtlas nodes.

Fig. 2. Mode of superimposition of salients to undisturbed shoreline.

Fig. 3. Standard definition sketch of the geometrical properties of salients applied to Maladroxia beach.

Fig. 4. Shoreline positions detected from photo interpretation and field survey, and locations of transects at Maladroxia beach.

Fig. 5. EPR values along 41 transects at Maladroxia beach and S/N band (±0.254 m/yr in red dotted lines).

Fig. 6a.No linear trend of shoreline position at the salient apex at Maladroxia beach.

Fig. 6b. Linear trend of shoreline position at on the Southern half of Maladroxia beach.

Fig. 7. *(S-Y)/B* vs. *B/S* for prediction of salient amplitude: comparison of plots from Hsu and Silvester (1990) in the lee of a single breakwater, Black and Andrews (2001) and Sardinian salients in the lee of submerged reefs and islands.

Fig. 8. Plot of *(S-Y)/B* vs. *B/S* for prediction of salient amplitude in the lee of an offshore obstacle, with a 95% of prediction interval.

Fig. 9. *Y/D* vs. *S/B:* database from Sunamura and Mizuno (1987) and Sardinian salients, and the "8 times rule".

Fig. 10. Plot of *D/B* vs. *B/S* for prediction of salient basal width in the lee of an offshore obstacle, with a 95% of prediction interval.

TABLES

Table 1. Geometrical properties values of the 13 salients along Sardinian coasts.

Table 2. Granulometric sand properties (median diameter and sorting), annual longshore component of the wave energy flux, and dominant wave and beach normal directions at the 13 salients.

Table3. Scale and accuracy of aerial imagery and IKONOS (2005) data.

Table4. Database for probabilistic model for shoreline change at the 13 beaches. Values in columns 6 and 7 are percentage of transects that fulfill both conditions (4) and (5) on S/N and CI methods.

	Latitude (N)	Longitude (E)	Configuration	B (m)	W (m)	Y (m)	S (m)	D (m)	P_L (m)	P_R (m)	B/S
Is Morus	38°56'40	8°57'2	S ; D ; A	46	152	33	80	362	145	85	0,57
Su Giudeu	38°53'1	8°51'48	E ; C ; Sy	99	103	88	174	566	260	275	0,57
Tuerredda	38°53'40	8°48'48	E ; C ; P	198	169	72	218	400	310	300	0,91
Maladroxia	38°59'57	8°26'57	S ; D ; P	177	145	17	45	150	80	90	3,93
Seu	39°58'32	8°23'30	S ; C ; A	79	146	59	128	406	140	165	0,61
Sa Mesa Longa	40°2'44	8°23'51	E ; D ; P	106	117	55	101	302	130	175	1,05
Platamona	40°49'10	8°27'59	S ; C ; Sy	439	63	29	142	589	142	142	3,10
Lu Bagnu	40°54'22	8°41'20	E ; D ; Sy	58	82	37	84	166	110	115	0,69
Tinnari	41°2'3	8°55'9	E ; C ; P	57	77	54	49	162	80	100	1,18
Vignola	41°7'40	9°3'45	S ; D ; Sy	71	82	54	68	318	80	90	1,03
Palau	41°7'30	9°26'24	E ; D ; A	27	23	15	24	30	45	50	1,15
Capo Comino	40°26'57	40°26'57	E ; D ; A	40	50	35	55	125	-	-	0,73
Feraxi	39°13'56	9°34'12	S ; D ; A	28	35	12	22	77	25	40	1,25

Table1. Geometrical properties values of the 13 salientsalong Sardinian coasts. Specifically, coordinates of salient apex in WGS84 latitude and longitude; geometric configuration of the salient/obstacle system (S: submerged obstacle; E: emergent obstacle; C: continuous obstacle; D: segmented obstacle; A: asymmetric salient; Sy: symmetric salient; P: pocket beach salient); P_L and P_R are the distances from the baseline of the diffraction points located on the left and on the right of a seaward observer).

	D_{50} (ϕ)	σ (ϕ)	$\dot{P}_{lbs}$ (W/m)	α_{dom} (°N)	α_n (°N)
Is Morus	1.064	0.495	232	135	150
Su Giudeu	1.447	0.504	200	135	145
Tuerredda	1.906	0.705	63	228	200
Maladroxia	2.178	0.516	37	151	90
Seu	0.012	0.509	2086	313	270
Sa Mesa Longa	-0.090	0.398	560	303	310
Platamona	1.450	0.456	1350	316	350
Lu Bagnu	-0.089	0.236	2473	318	330
Tinnari	-0.456	0.152	1190	303	350
Vignola	1.564	0.568	1970	360	360
Palau	-0.128	0.238	57	44	80
Capo Comino	1.350	0.510	232	147	110
Feraxi	0.568	0.426	140	140	110

Table2.Granulometric sand properties (median diameter and sorting), annual longshore component of the wave energy flux, and dominant wave and beach normal directions at the 13 salients.

Year	Scale	Δ_h(m)
1954	25000	10.0
1968	10000	2.5
1977	10000	2.5
1997	10000	5.0
2000	10000	5.0
2003	10000	5.0
2005	10000	4.0
2006	10000	5.0
2008	2000	1.0

Table3. Scale and accuracy ofaerial imagery and IKONOS (2005) data.

	N_{yy}	S/N (m/yy)	N_t	d (m)	% (4)	% (5)
Is Morus	9	0.254	22	8	100.0	81.8
Su Giudeu	11	0.254	63	8	80.9	85.7
Tuerredda	10	0.123	41	8	81.9	85.4
Maladroxia	12	0.254	41	4	95.2	80.4
Seu	8	0.254	54	8	100.0	94.4
Sa Mesa Longa	8	0.333	36	8	100.0	83.3
Platamona	8	0.123	54	8	90.7	94.4
Lu Bagnu	9	0.254	19	8	94.7	100.0
Tinnari	10	0.254	34	5	100.0	82.4
Palau	9	0.254	14	8	92.9	85.7
Vignola	9	0.167	41	8	100.0	100.0
Capo Comino	10	0.254	38	8	84.2	60.8
Feraxi	8	0.123	19	5	84.2	84.2

Table4. Database for probabilistic model for shoreline change at the 13 beaches.Values in columns 6 and 7 are percentage of transects that fulfill both conditions (4) and (5) on S/N and CI methods.

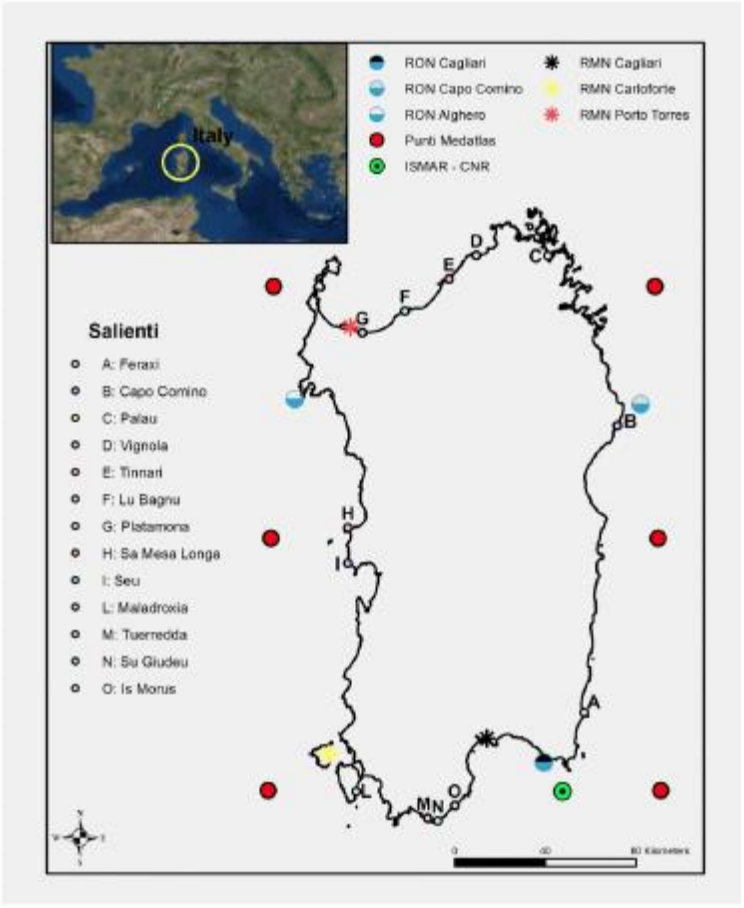

Fig. 1. Map of the island of Sardinia showing locations of the 13 salients, RON and RMN gauges, and MedAtlas and ISMAR-CNR nodes.

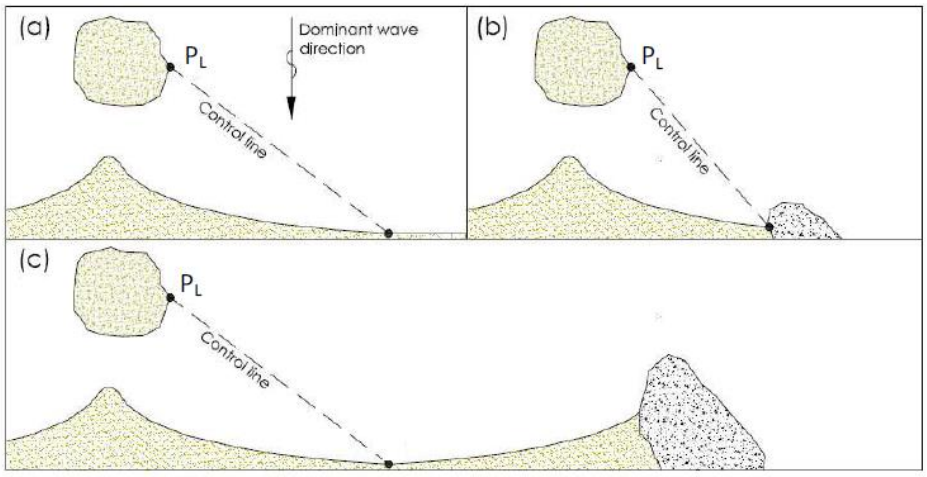

Fig. 2. Mode of superimposition of salients to undisturbed shoreline.

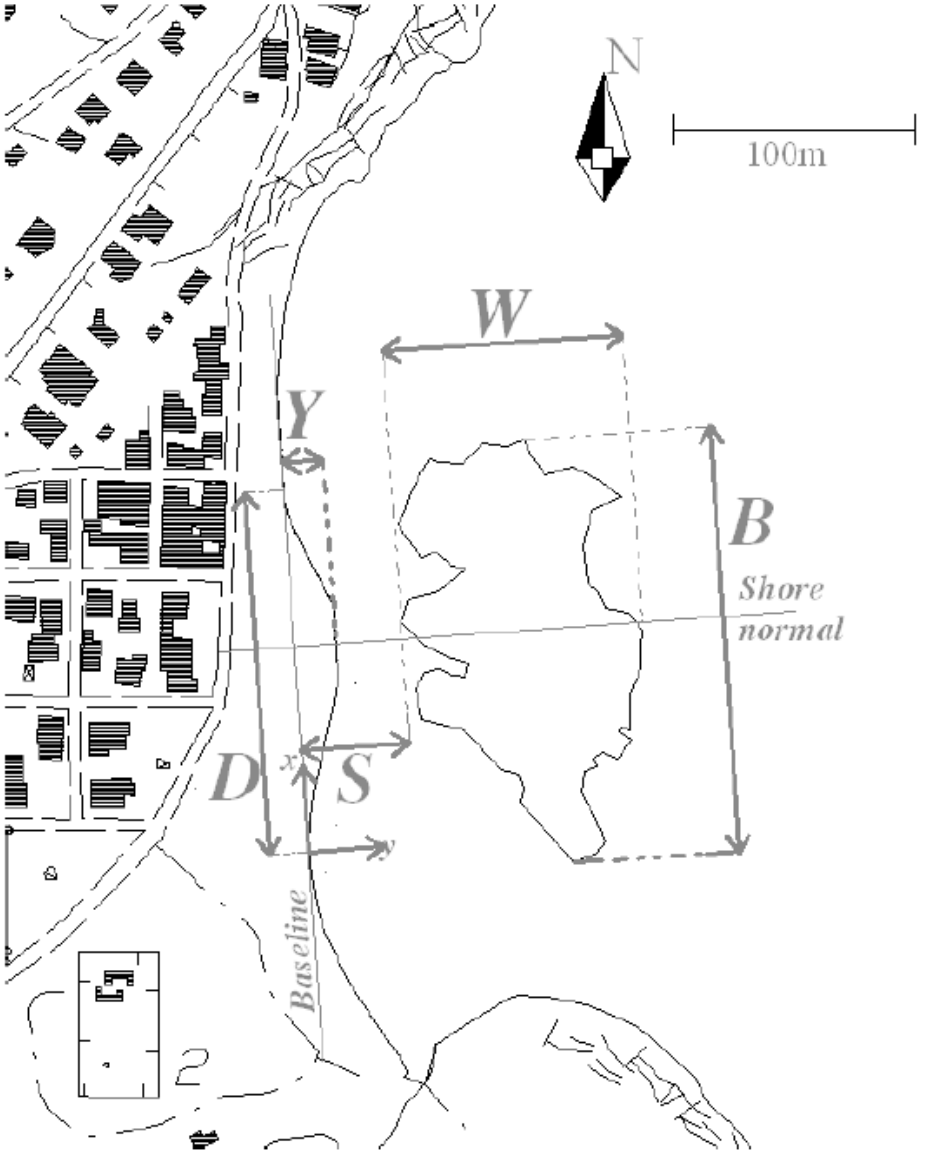

Fig. 3. Standard definition sketch of the geometrical properties of salients applied to Maladroxia beach.

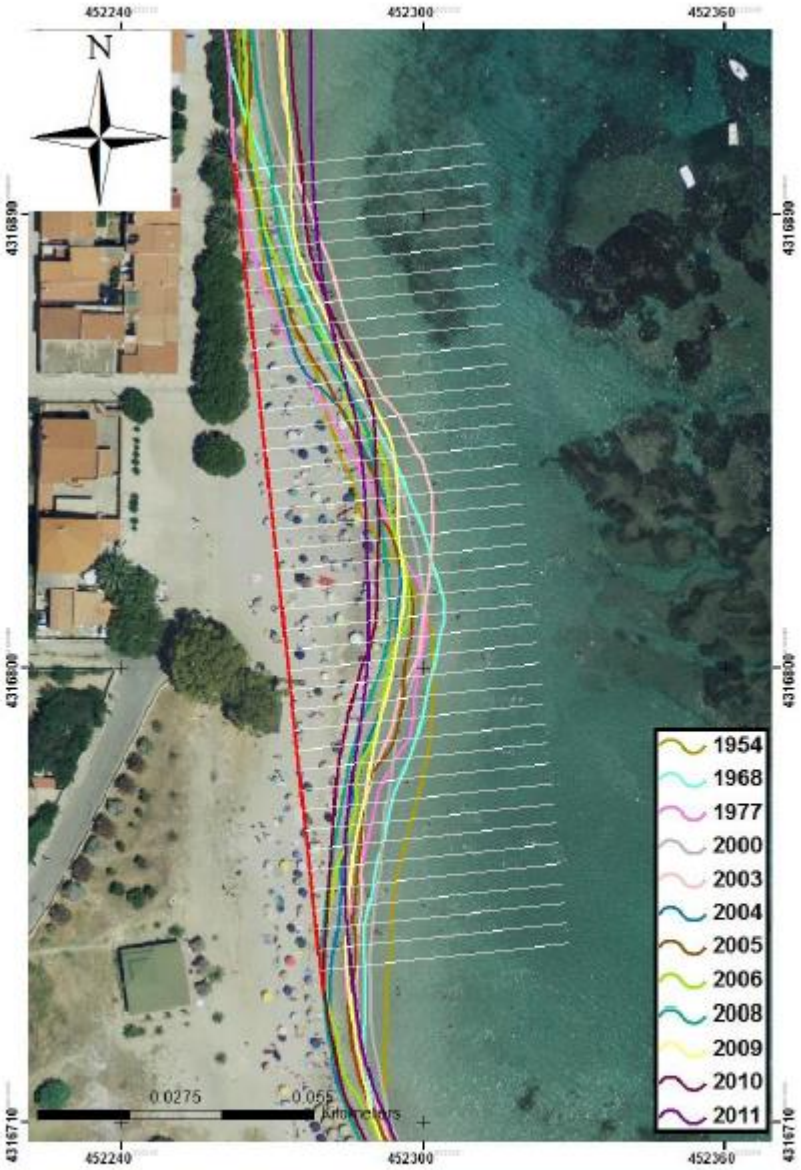

Fig. 4. Shoreline positions detected from photo interpretation and field survey, and locations of transects at Maladroxia beach.

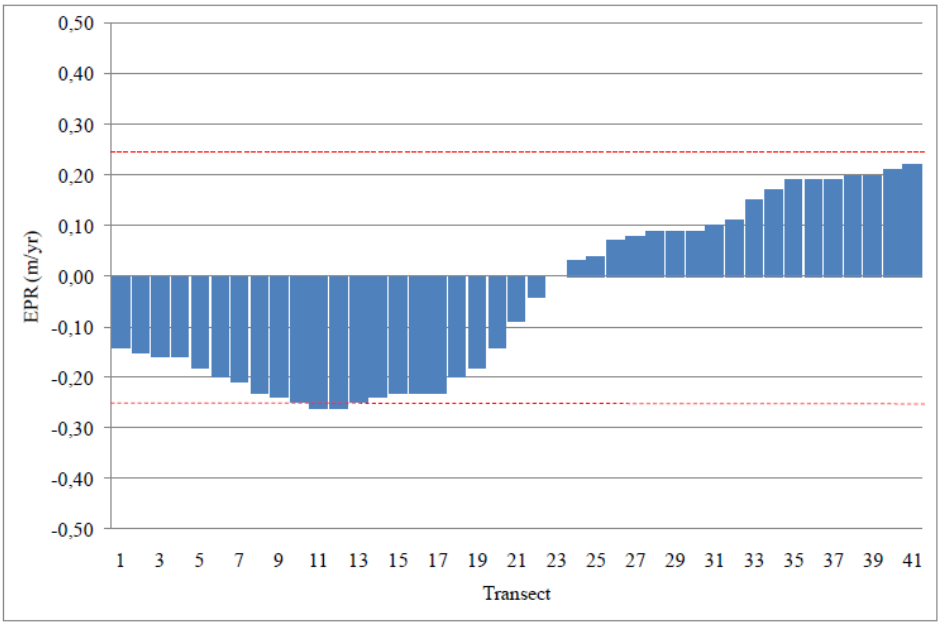

Fig. 5. EPR values along 41 transects at Maladroxia beach and S/N band (±0.254 m/yr in red dotted lines).

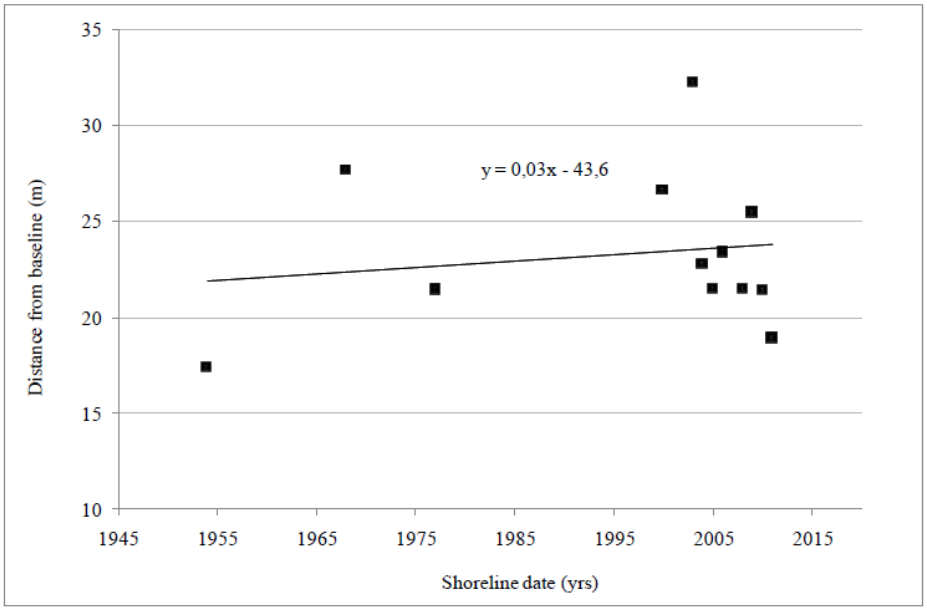

Fig. 6a. No linear trend of shoreline position at the salient apex at Maladroxia beach.

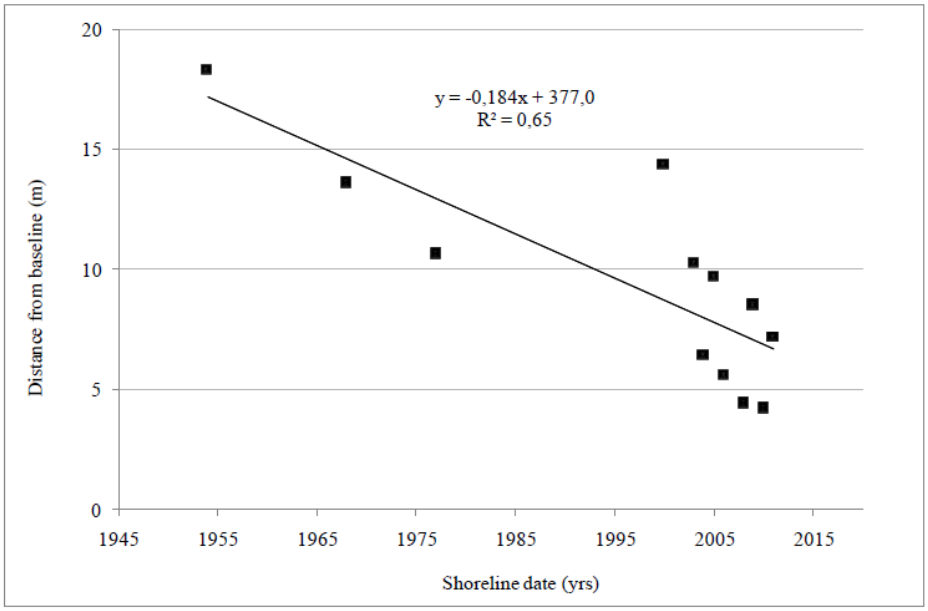

Fig. 6b. Linear trend of shoreline position at on the Southern half of Maladroxia beach.

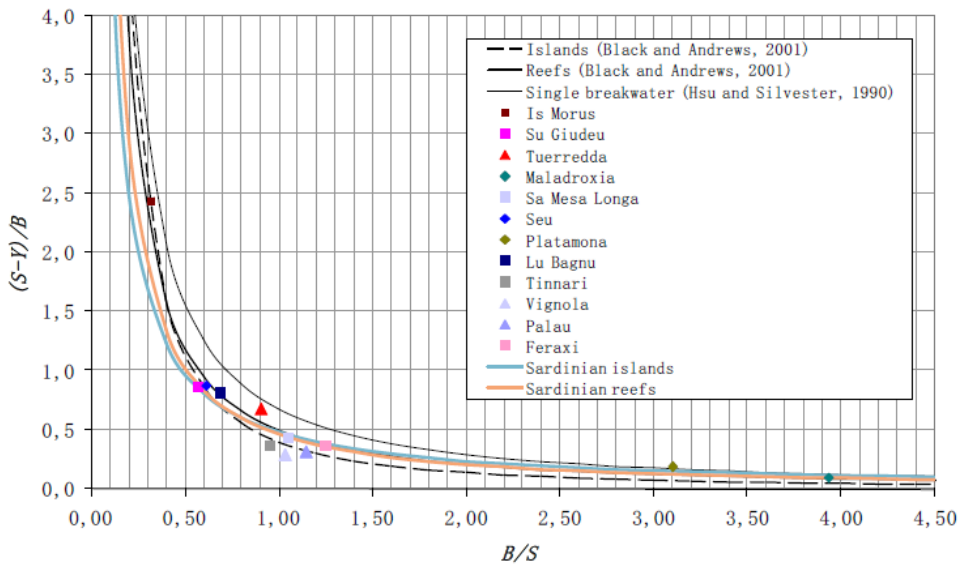

Fig. 7. *(S-Y)/B* vs. *B/S* for prediction of salient amplitude: comparison of plots from Hsu and Silvester (1990) in the lee of a single breakwater, Black and Andrews (2001) and Sardinian salients in the lee of submerged reefs and islands.

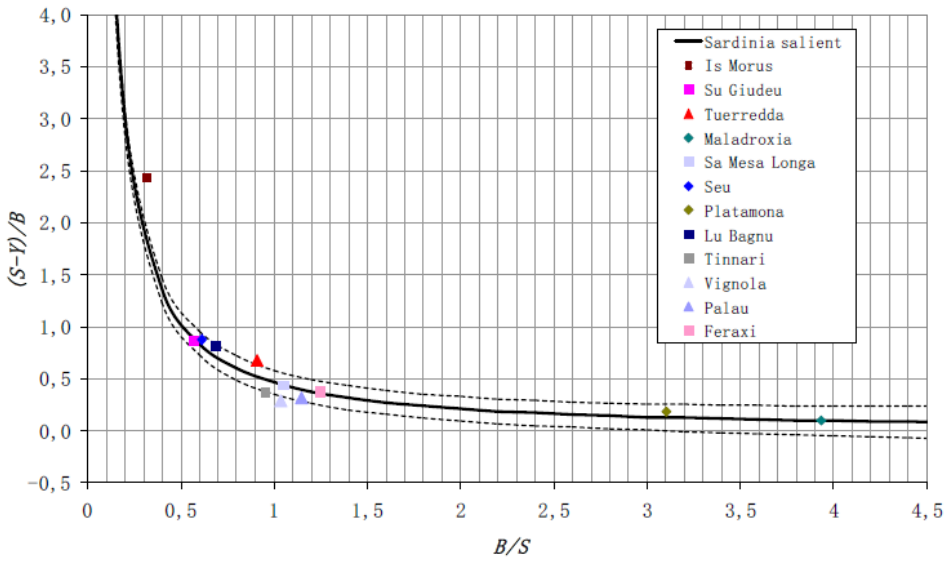

Fig. 8. Plot of *(S-Y)/B* vs. *B/S* for prediction of salient amplitude in the lee of an offshore obstacle, with a 95% of prediction interval.

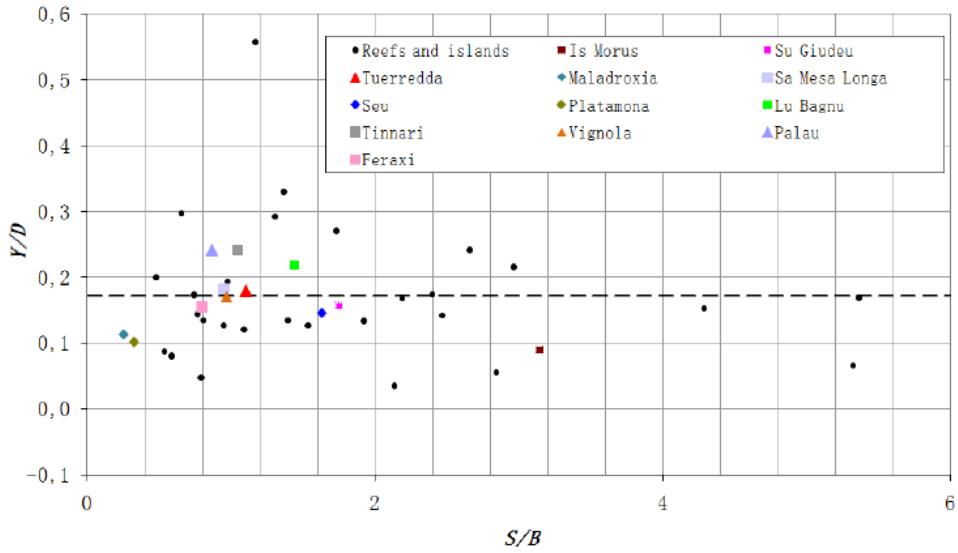

Fig. 9. *Y/D* vs. *S/B:* database from Sunamura and Mizuno (1987) ("reefs and islands" points) and Sardinian salients, and the "8 times rule".

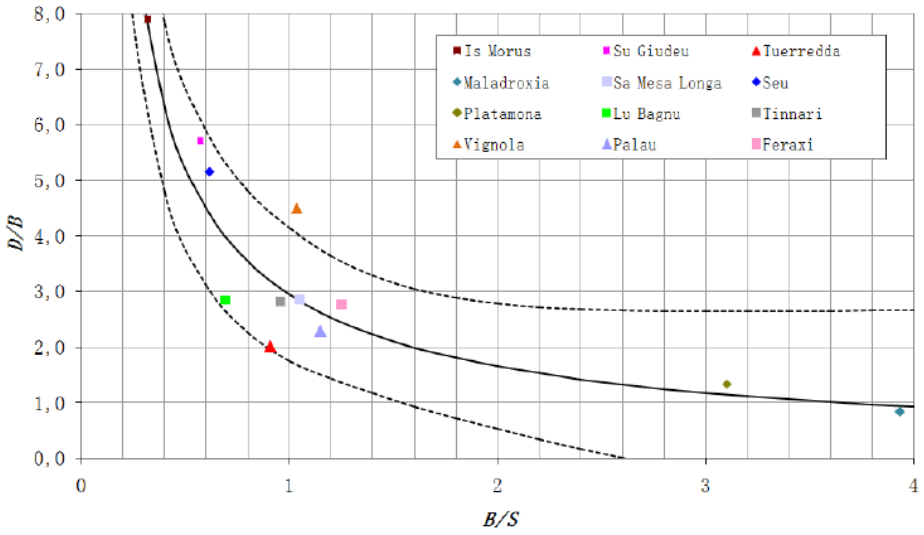

Fig. 10. Plot of *D/B* vs. *B/S* for prediction of salient basal width in the lee of an offshore obstacle, with a 95% of prediction interval.